DOI: 10.1002/chem.200802660

Synthesis, Structure, and Physico-optical Properties of Manganate(II)-Based Ionic Liquids

Slawomir Pitula and Anja-Verena Mudring*[a]

Abstract: Several ionic liquids (ILs) based on complex manganate(II) anions with chloro, bromo, and bis(trifluoromethanesulfonyl)amido (Tf_2N) ligands have been synthesized. As counterions, *n*-alkyl-methylimidazolium ($C_n$mim) cations of different chain length (alkyl = ethyl (C_2), propyl (C_3), butyl (C_4), hexyl (C_6)) were chosen. Except for the 1-hexyl-3-methylimidazolium ILs, all of the prepared compounds could be obtained in a crystalline state at room temperature. However, each of the compounds displayed a strong tendency to form a supercooled liquid. Generally, solidification via a glass transition took place below −40 °C. Consequently, all of these compounds can be regarded as ionic liquids. Depending on the local coordination environment of Mn^{2+}, green (tetrahedrally coordinated Mn^{2+}) or red (octahedrally coordinated Mn^{2+}) luminescence emission from the $^4T(G)$ level is observed.[1] The local coordination of the luminescent Mn^{2+} centre has been unequivocally established by UV/Vis as well as Raman and IR vibrational spectroscopies. Emission decay times measured at room temperature in the solid state (crystalline or powder) were generally a few ms, although, depending on the ligand, values of up to 25 ms were obtained. For the bromo compounds, the luminescence decay times proved to be almost independent of the physical state and the temperature. However, for the chloro- and bis(trifluoromethanesulfonyl)amido ILs, the emission decay times were found to be dependent on the temperature even in the solid state, indicating that the measured values are strongly influenced by nuclear motion and the vibration of the atoms. In the liquid state, the luminescence of tetrahedrally coordinated Mn^{2+} could only be observed when the tetrachloromanganate ILs were diluted with the respective halide ILs. However, for $[C_3mim][Mn(Tf_2N)_3]$, in which Mn^{2+} is in an octahedral coordination environment, a weak red emission from the pure compound was found even in the liquid state at elevated temperatures.

Keywords: imidazolium cations · ionic liquids · luminescence · manganates · transition metals

Introduction

Mn^{2+} is known to exhibit interesting photophysical properties such as fluorescence and phosphorescence. Well-known phosphors include $[Zn(Mn)]_2SiO_4$,[1] but, depending on the coordination environment, either green (tetrahedrally coordinated Mn^{2+}) or red to pink (octahedrally coordinated Mn^{2+}) luminescence can also be observed from simple halogenido complexes.[2,3] Besides photoluminescence, triboluminescence[4,5] as well as electroluminescence[6–11] have also been observed for certain tetraalkylammonium salts. In a high proportion of the studied optically active manganate(II) salts, the counter cations have been organic ammonium ions. Often, they conform to the general composition $[NR_4][MnX_4]$ (R = H, alkyl; X = Cl, Br, I). This composition is strongly reminiscent of recently studied tetrachloroferrate ionic liquids such as $[C_4mim][FeCl_4]$,[12–17] which with Fe^{3+} also contain a d^5 ion. Because of their high single-ion magnetism, they can be manipulated by an external magnetic field.[18]

In general, as salt-like compounds with low melting points (usually below 100 °C), ionic liquids offer the possibility of engineering their properties to meet the needs of a particular application through appropriate choice of the combination of cation and anion.[19] In the case of complex manganate salts, this has already been realized by Seddon and Earle, who suggested that complex manganate anions in combination with organic cations might be interesting light-emitting materials for use in cathode-ray tubes, fluorescent tubes, X-ray imaging screens, and radiation detectors, as

[a] Dr. S. Pitula, Prof. Dr. A.-V. Mudring
Anorganische Chemie I - Festkörperchemie und Materialien
Ruhr-Universität Bochum, 44780 Bochum (Germany)
Fax: (+49) 234-32-14951
E-mail: anja.mudring@rub.de

Supporting information for this article is available on the WWW under http://dx.doi.org/10.1002/chem.200802660.

well as in toys, signs, and so on.[20] However, all but one of the reported compounds were solid at room temperature and unfortunately lost their luminescent properties on reaching temperatures at which solid–solid phase transitions or melting occurred.

Recently, we were able to show that low-melting compounds composed of an organic cation and an optically active rare-earth ion, for example $[C_4mpyr]_2[Pr(Tf_2N)_5]$ (mpyr = *N*-methyl-*N*-propylpyrrolidinium);[21] $[C_3mim][Eu(Tf_2N)_4]$, $[C_4mim][Eu(Tf_2N)_5]$, and $[C_4mpyr][Eu(Tf_2N)_5]$;[22] and $[C_4mim]_{3-x}[Dy(SCN)_{8-x}(H_2O)_x]$,[23] exhibit excellent luminescent properties. For these systems, unexpectedly good luminescent properties can even be maintained in the molten/liquid state due to the favourable coordination environment of the lanthanide ion. Furthermore, replacement of conventional solvents by carefully designed ionic liquids can generally lead to dramatic increases in the emission decay of the excited state and the quantum yields of emission, even for NIR luminescence.[24,25]

In continuation of our research, we have sought ionic liquid transition metal systems with interesting luminescent properties in the (ionic) liquid state.

Experimental Section

Materials: The following chemicals were used as received unless mentioned otherwise. Acetonitrile (>99.5%), dichloromethane (99.6%), toluene (99.5%), manganese(II) carbonate, manganese(II) bromide (98%), 1-bromobutane (>99%), 1-chlorohexane (99%), and lithium bis(trifluoromethylsulfonyl)amide (>99%) were purchased from Sigma–Aldrich (Steinheim, Germany). Ethyl acetate (99.8%) was obtained from KMF (St. Augustin, Germany). 2-Propanol (extra dry), methanol (extra dry), bromoethane (98%), 1-bromopropane (98%), 1-chlorobutane (>99%), 1-chloropropane (99%), and 1-bromohexane (>98%) were purchased from Acros (Geel, Belgium). *N*-Methylimidazole (>99%) was purchased from Acros (Geel, Belgium), dried over elemental sodium, and distilled prior to use. Chloroethane (for synthesis) was purchased from Merck (Hohenbrunn, Germany).

Syntheses

HTf_2N: HTf_2N was obtained by sublimation from a solution of $LiTf_2N$ in excess sulfuric acid. The reaction mixture was stirred for 2 days at 80–100°C. The colorless product crystallized upon cooling the vapour in yields of about 90%. ^{1}H NMR (300 MHz, D_2O): $\delta = 4.77$ ppm (s, 1H); ^{19}F NMR (300 MHz, D_2O): $\delta = -79.16$ ppm (s, 6F); ^{13}C{^{19}F} NMR (300 MHz, D_2O): $\delta = 19.27$ ppm (s, 2C).

$Mn(Tf_2N)_2$: Manganese(II) carbonate was suspended in water and an equimolar amount of HTf_2N dissolved in water was added dropwise. The reaction mixture was stirred at 60–80°C for 2 h. The water was then evaporated and the product was dried at 140°C under reduced pressure for 1 day. The crude product was resublimed at 300°C. Elemental analysis calcd (%): C 7.80, H 0.00, N 4.55, S 20.81; found: C 7.78, H 0.10, N 4.64, S 21.40.

$MnCl_2$: Manganese(II) carbonate was suspended in water, an excess of hydrochloric acid was added, and the mixture was stirred at 120°C until a pink solid precipitated as a slurry. The crude product was dried at 300°C under reduced pressure for two days to give pink $MnCl_2$. The purity of the obtained product was confirmed by powder XRD analysis.

General procedure for the synthesis of 1-*n*-alkyl-3-methylimidazolium chlorides and bromides: Generally, the chloride and bromide ILs were synthesized by alkylation of *N*-methylimidazole with the appropriate haloalkane.[21,24] For all ILs of the type $C_n$mimBr/Cl ($n = 2, 3, 4$), but not for C_6mimBr and C_6mimCl, a white crystalline powder was obtained.

C_2mimCl was synthesized by adding a fourfold excess of cold chloroethane to dry *N*-methylimidazole in a Teflon cartridge (Parr Instruments Co., Illinois, USA). The filled Teflon cartridge was inserted into an autoclave (Parr Instruments Co., Illinois, USA) and the contents were stirred at 90°C for four days. The reaction mixture was then allowed to cool to room temperature and the excess chloroethane was evaporated. The very hygroscopic white powder obtained was dried at 95°C under reduced pressure for several days.

C_2mimCl: ^{1}H NMR (300 MHz, D_2O): $\delta = 1.46$ (t, 3H), 3.87 (s, 3H), 4.21 (q, 2H), 7.45 (d, 2H), 8.72 ppm (s, 1H).

C_3mimCl: ^{1}H NMR (300 MHz, D_2O): $\delta = 0.85$ (t, 3H), 1.81 (q, 2H), 3.83 (s, 3H), 4.09 (t, 2H), 7.39 (d, 2H), 8.66 ppm (s, 1H).

C_4mimCl: ^{1}H NMR (300 MHz, D_2O): $\delta = 0.82$ (t, 3H), 1.18 (m, 2H), 1.72 (quint., 2H), 3.76 (s, 3H), 4.01 (t, 2H), 7.30 (d, 2H), 8.57 ppm (s, 1H).

C_6mimCl: ^{1}H NMR (300 MHz, D_2O): $\delta = 0.78$ (t, 3H), 1.22 (m, 6H), 1.80 (t, 2H), 3.83 (s, 3H), 4.13 (t, 2H), 7.40 (d, 2H), 8.67 ppm (s, 1H).

C_2mimBr: ^{1}H NMR (300 MHz, $CDCl_3$): $\delta = 1.23$ (t, 3H), 3.75 (s, 3H), 4.06 (q, 2H), 7.39 (s, 2H), 9.82 ppm (s, 1H).

C_3mimBr: ^{1}H NMR (300 MHz, $CDCl_3$): $\delta = 0.44$ (t, 3H), 1.45 (sext., 2H), 3.61 (s, 3H), 3.82 (t, 2H), 7.82 (d, 2H), 9.67 ppm (s, 1H).

C_4mimBr: ^{1}H NMR (300 MHz, $CDCl_3$): $\delta = 0.85$ (t, 3H), 1.27 (sext., 2H), 1.81 (quint., 2H), 4.02 (s, 3H), 4.24 (t, 2H), 7.56 (d, 2H), 10.19 ppm (s, 1H).

C_6mimBr: ^{1}H NMR (300 MHz, $CDCl_3$): $\delta = 0.75$ (t, 3H), 1.20 (m, 6H), 1.81 (quint., 2H), 2.05 (s, 2H), 4.03 (s, 3H), 4.22 (t, 2H), 7.55 (d, 2H), 10.24 ppm (s, 1H).

General procedure for the synthesis of 1-*n*-alkyl-3-methylimidazolium bis(trifluoromethanesulfonyl)amides: The 1-*n*-alkyl-3-methylimidazolium bis(trifluoromethanesulfonyl)amides were synthesized by metathesis reactions of the 1-*n*-alkyl-3-methylimidazolium halides with lithium bis(trifluoromethanesulfonyl)amide.[19,21,24]

$[C_2mim][Tf_2N]$: ^{1}H NMR (300 MHz, $CDCl_3$): $\delta = 1.58$ (t, 3H), 4.06 (q, 2H), 7.73 (d, 2H), 9.00 ppm (s, 1H); ^{19}F NMR (300 MHz, $CDCl_3$): $\delta = -79.96$ ppm (s, 6H).

$[C_3mim][Tf_2N]$: ^{1}H NMR (300 MHz, $CDCl_3$): $\delta = 0.87$ (t, 3H), 1.82 (sext., 2H), 3.84 (s, 3H), 4.05 (t, 2H), 7.29 (d, 2H), 8.53 ppm (s, 1H); ^{19}F NMR (300 MHz, $CDCl_3$): $\delta = -79.43$ ppm (s, 6H).

$[C_4mim][Tf_2N]$: ^{1}H NMR (300 MHz, $CDCl_3$): $\delta = 0.89$ (t, 3H), 1.31 (sext., 2H), 1.80 (quint., 2H), 3.87 (s, 3H), 4.11 (t, 2H), 7.30 (d, 2H), 8.59 ppm (s, 1H); ^{19}F NMR (300 MHz, $CDCl_3$): $\delta = -79.32$ ppm (s, 6H).

$[C_6mim][Tf_2N]$: ^{1}H NMR (300 MHz, $CDCl_3$): $\delta = 0.83$ (t, 3H), 1.26 (m, 6H), 1.81 (quint., 2H), 3.87 (s, 3H), 4.11 (t, 2H), 7.30 (d, 2H), 8.61 ppm (s, 1H); ^{19}F NMR (300 MHz, $CDCl_3$): $\delta = -79.27$ ppm (s, 6H).

General procedure for the synthesis of bis(1-alkyl-3-methylimidazolium) tetrahalogenomanganates: According to $2\ RmimX + MnX_2 \rightarrow [Rmim]_2[MnX_4]$ (R = alkyl; X = Cl, Br), equimolar amounts of the appropriate dry 1-alkyl-3-methylimidazolium halide and MnX_2 were placed in a Schlenk tube and heated to 80°C. After completion of the reaction, which could be monitored visually by the complete dissolution of MnX_2, the product was kept at 90°C under reduced pressure for one day. In all cases, the yield of the yellow-green to brownish ionic liquid was quantitative. Each liquid product was washed several times with 2-propanol to remove unreacted starting materials. Alternatively, the reaction could be performed in anhydrous methanol or 2-propanol, with subsequent crystallization of the products after removal of the solvent. The halide compounds were purified by washing several times with 2-propanol and repeatedly recrystallizing from 1:0.5→1:1 methanol/2-propanol mixtures.

$[C_2mim]_2[MnCl_4]$: Elemental analysis calcd (%): C 34.39, H 5.29, N 13.37; found: C 34.26, H 5.49, N 13.34.

$[C_3mim]_2[MnCl_4]$: Elemental analysis calcd (%): C 37.75, H 5.89, N 12.59; found: C 37.67, H 6.20, N 12.48.

$[C_4mim]_2[MnCl_4]$: Elemental analysis calcd (%): C 40.44, H 6.36, N 11.79; found: C 40.36, H 6.37, N 11.63.

$[C_6mim]_2[MnCl_4]$: Elemental analysis calcd (%): C 45.21, H 7.21, N 10.55; found: C 44.71, H 7.77, N 10.25.

$[C_2mim]_2[MnBr_4]$: Elemental analysis calcd (%): C 24.15, H 3.72, N 9.39; found: C 24.51, H 3.48, N 9.45.

$[C_3mim]_2[MnBr_4]$: Elemental analysis calcd (%): C 26.91, H 4.19, N 8.97; found: C 26.90, H 4.30, N 8.94.

$[C_4mim]_2[MnBr_4]$: Elemental analysis calcd (%): C 29.59, H 4.66, N 8.63; found: C 29.71, H 4.70, N 8.65.

$[C_6mim]_2[MnBr_4]$: Elemental analysis calcd (%): C 33.88, H 5.40, N 7.90; found: C 33.23, H 5.44, N 7.72.

General procedure for the synthesis of 1-alkyl-3-methylimidazolium tris-[bis(trifluoromethanesulfonyl)amide]manganates(II): According to $RmimTf_2N + Mn(Tf_2N)_2 \rightarrow [Rmim][Mn(Tf_2N)_3]$ (R = alkyl), the appropriate 1-alkyl-3-methylimidazolium bis(trifluoromethanesulfonyl)amide ionic liquid was placed in a Schlenk tube and anhydrous $Mn(Tf_2N)_2$ was added. The mixture was then dissolved in anhydrous acetonitrile and stirred for one to two days at 60 °C. After completion of the reaction, the solvent was removed and the product was dried under reduced pressure for two days at 80 °C. In all cases, the yield of the product was quantitative.

$[C_2mim][Mn(Tf_2N)_3]$: Elemental analysis calcd (%): C 14.32, H 1.10, N 6.96, S 19.10; found: C 14.67, H 1.30, N 7.00, S 18.54; IC (Br^-): 119.6 ppm.

$[C_3mim][Mn(Tf_2N)_3]$: Elemental analysis calcd (%): C 15.30, H 1.28, N 6.86, S 18.85; found: C 15.21, H 1.16, N 6.88, S 19.01; IC (Br^-): 110.6 ppm.

$[C_4mim][Mn(Tf_2N)_3]$: Elemental analysis calcd (%): C 16.25, H 1.46, N 6.77, S 18.56; found: C 16.85, H 2.90, N 5.23, S 18.36; IC (Br^-): 126.4 ppm.

$[C_6mim][Mn(Tf_2N)_3]$: Elemental analysis calcd (%): C 18.08, H 1.80, N 6.59, S 18.11; found: C 17.88, H 2.82, N 6.70, S 17.35; IC (Br^-): 113.3 ppm.

Thermal investigations: Differential scanning calorimetry (DSC) was performed with a Netzsch Phoenix DSC 204 F1 thermal analyzer with argon as the protective gas. On average, 10–15 mg of a sample was placed in an aluminium pan, which was then cold-sealed with an aluminium lid under argon in a dry box. For the measurement, the aluminium lid was pierced inside the calorimeter under an argon stream to allow for thermal expansion. A typical DSC run involved heating to 100–120 °C at a rate of 5 K min^{-1} and subsequent cooling to −100 °C at 5 K min^{-1}. The experimental data are displayed in such a way that exothermic peaks occur at negative heat flow and endothermic peaks at positive heat flow.

UV/Vis/NIR spectra: UV/Vis/NIR absorption spectra were measured at room temperature on a Varian Cary 05E spectrometer (Varian, Palo Alto, USA). Samples of the compounds were placed in silica cuvettes under inert conditions (dry box) and the cuvettes were sealed with Parafilm (Menasha, WI, USA). All compounds were diluted with the corresponding alkylimidazolium halide IL, as otherwise their absorbances were too high.

Luminescence spectroscopy: Excitation and emission photoluminescence spectra were recorded at room temperature on a Fluorolog 3 spectrometer (Horiba Jobin Yvon GmbH, München, Germany) with a 450 W xenon lamp as a steady-state excitation source, a double-excitation monochromator, an emission monochromator, and a photomultiplier for detection. For emission decay measurements, a chopper system was used to create light flashes. The excitation and emission slits of the source and the detector were adjusted for each different sample. The delay between the light flash of the source and the detector opening was chosen in such a way that a negligible intensity of the residual light was obtained. Typically, the initial delay was chosen to be 50 μs or more. The detection time was tuned to be about 5–10 times the duration of the estimated emission decay. These parameters were also chosen when recording the phosphorescence spectra of the respective samples.

Electronic transitions were assigned according to the Tanabe–Sugano energy-level diagrams of d^5 ions[26–29] and by comparison with recent literature data. Luminescence emission decay times were determined by measurement of the luminescence intensity decay curves.

Generally, photoluminescence spectra were recorded at liquid nitrogen temperature as well as at room temperature. In the cases of $[C_3mim]_2[MnCl_4]$, $[C_3mim]_2[MnCl_4]$, and $[C_3mim][Mn(Tf_2N)_3]$, the temperature dependence of the luminescence decay was measured using an outer silica cuvette filled with deionized water. Here, temperature control was achieved by means of a Julabo FP-50 cryostat. The accuracy of the temperature stability of the sample holder was appraised by a fitted calibration curve to be about ±0.1 °C. After reaching the requisite temperature, the sample was equilibrated for 10–15 min.

Vibrational spectroscopy: IR spectra of the ILs were recorded using an IFS-66 V-S Fourier-transform IR spectrometer; samples were ground to a fine powder and pressed into pellets of KBr (mid-IR region) or polyethylene (far-IR region). Raman spectra were measured on an FRA 106-S Fourier-transform Raman spectrometer. Under inert conditions, the samples were introduced into quartz capillaries with an inner diameter of 3 mm, which were subsequently sealed with an air-tight screw cap.

Triboluminescence: Triboluminescence was tested by rubbing crystalline samples with a glass rod. For visual observation of triboluminescence, it proved to be advantageous to cool the samples with liquid nitrogen.

Electroluminescence: A reduced pressure of 10^{-5} bar was applied to a Schlenk tube containing the Mn IL. On applying a high-frequency generator beam (20 W, 0.91 A, 220 V, type VP 20 a), luminescence was observed.

Elemental analyses: Elemental analyses were performed using a Euro Vektor CHNS-O EA3000 analyzer. The samples were sealed in small tin tubes inside a glove box.

NMR: All NMR spectra were recorded on a Bruker DPX AC 300 spectrometer with an automatic sample changer.

Ion chromatography: Ion chromatography was performed with a Metrohm 881 compact IC.

Results and Discussion

Thermal analysis: Thermal data for the investigated manganate(II) complex compounds are compiled in Table 1. Graphical representations of all of the DSC thermograms, together with detailed information on the transition enthalpies, are collected in the Supporting Information. For all DSC scans, the heating and cooling cycles were repeated twice to check for any changes in the thermal properties in the second cycle. In fact, for all compounds the second cycles exactly reproduced the first, unless stated otherwise.

The investigated compounds all proved to be true ionic liquids. All short-chain (C_2–C_4) compounds could be obtained as crystalline samples, whereas those with a C_6 chain showed an extremely strong tendency to supercool and solidify as glasses. Thus, none of the 1-hexyl-3-methylimidazolium manganate compounds could be crystallized, neither by homogeneous nor by heterogeneous crystallization techniques.

Three different types of thermal behaviour could be observed for the studied ILs. In the first type (Figure 1, left), as seen for the 1-ethyl- and 1-propyl-3-methyl-imidazolium halide-containing ILs, distinct melting points upon heating and distinct crystallization temperatures upon cooling were observed.[30] A typical DSC scan for this kind of IL is illustrated in Figure 1. Thermal events occurring at temperatures lower than the melting point can be attributed to solid–solid

Table 1. Thermal data acquired by DSC measurements of 1-*n*-alkyl-3-methylimidazolium manganate(II) ionic liquids. Data are given in °C.

Compound	Cooling			Heating			
	glass transition	crystallization	solid–solid phase transition	glass transition	crystallization	melting	solid–solid phase transition
$[C_2mim]_2[MnCl_4]$	–	39.2	14.8	–		77.3	–
$[C_3mim]_2[MnCl_4]$	−65.8	−7.8	−27.5	−54.4	−35.5		–
$[C_4mim]_2[MnCl_4]$	−54.0	–	–	−49.2		62.0	–
$[C_6mim]_2[MnCl_4]$	−51.8	–	–	−50.1			–
$[C_2mim]_2[MnBr_4]$	–	39.5	–	–	10.2	72.0	–
$[C_3mim]_2[MnBr_4]$	–	18.2	−54.1	–	−10.4	53.8	−24.8
$[C_4mim]_2[MnBr_4]$	−55.4	–	–	−49.9		44.2	–
$[C_6mim]_2[MnBr_4]$	−54.2	–	–	−49.5			–
$[C_2mim][Mn(Tf_2N)_3]$	−45.2	–		−47.2	22.7		–
$[C_3mim][Mn(Tf_2N)_3]$	−44.4	–	–	−44.1		36.7	0.7
$[C_4mim][Mn(Tf_2N)_3]$	−48.5	–	–	−40.3		66.0	–
$[C_6mim][Mn(Tf_2N)_3]$	−56.4	–	–	−50.8			–

phase transitions. In some cases, the samples partially solidified as a glass and recrystallized upon heating before melting. The tendency to solidify as a glass becomes more and more pronounced with increasing length of the alkyl chain.

Second, in the case of the 1-butyl-3-methylimidazolium ILs, after melting of the crystalline material (which was obtained by crystallization from solution) to the liquid state, only glass transitions could be observed upon cooling the samples (Figure 1, middle). After repeated heating, these glasses formed supercooled liquids, which showed no tendency for homogeneous crystallization. Finally, the 1-hexyl-3-methylimidazolium ILs could not even be crystallized from solution (Figure 1, right). ILs of this third type have no real melting or freezing points, and only glass transitions are observed.

Extension of the alkyl chain from C_2 to C_3 leads in the case of the tetrahalogenomanganates to a depression of the melting point. Further extension of the alkyl chain seems to inhibit the crystallization. Hence, with longer alkyl chains, the formation of a glass is preferred. Not only an extension of the alkyl chain of the cation, but also a change of the anion from the more symmetric halide to the less symmetric bis(trifluoromethanesulfonyl)amide, favours solidification as a glass. In both cases, packing frustrations seem to be the main reason for this behaviour. The less symmetric the cation, the greater the tendency to form a glass rather than a crystalline material.

Infrared and Raman spectroscopies: The expected vibrations of the imidazolium ring are clearly visible in the infrared and Raman spectra of the Mn-based ILs (see Figure 2 and the Supporting Information). The CH deformation modes can be found in the range 1300–1550 cm^{-1}, the CH stretching modes in the range 2800–3200 cm^{-1}, and the CH rocking mode at 720 cm^{-1}. All vibrational modes of the respective cations of the manganese-containing ILs found in the mid-IR region correlate well with those of the respective neat halide ILs. In other words, no significant influence of the anion on the counter cation was found.

Metal–ligand vibrations of tetrahedrally coordinated Mn^{2+} are infrared- and Raman-active, whilst for the octahedrally coordinated compounds the respective modes are only Raman-active. Such metal–ligand vibrations are usually observed in the far-IR region, between 200 and 400 cm^{-1}. In the far-IR region, the sharp Mn−Cl stretching mode typically has its maximum absorbance at around 290 cm^{-1}, sometimes accompanied by shoulders at lower or higher frequencies, while the Mn−Br mode appears as a broad band at 220 cm^{-1} (see Figure 2a). The bromo compounds exhibit a much lower absorbance intensity in the far-IR spectra than the corresponding chloro compounds. The symmetric Mn–halide vibrations in Figure 2d are marked with arrows. Typical values of ν_s (Mn−Cl) and ν_s (Mn−Br) are 255 cm^{-1} and 160 cm^{-1}, respectively, which are in agreement with those reported in the literature.[31–42] Generally, these Mn–halide vibrations have only weak intensities and typically appear in the region below 400 cm^{-1}.[43]

As all of the Tf_2N derivatives of the Mn-based ILs proved to be optically dense, their mid-IR spectra had to be recorded from solutions of the respective room temperature liquid ILs to trace any transmission. As can be seen in Figure 2c, only $[C_6mim][Mn(Tf_2N)_3]$ showed a significant transmission. Compared to the tetrahalogeno ILs, the Tf_2N derivatives do not exhibit such pronounced fine splitting of their bands. The bands for the CH stretching and deformation modes exhibit a much lower intensity than is observed in the spectra of the respective halide ILs. The ν_s (S−N−S) mode at 748 cm^{-1} for the Tf_2N Mn^{2+} derivatives is shifted by about 20 cm^{-1} to lower wavenumber compared to the ν_s (S−N−S) mode of HTf_2N at 767 cm^{-1}, but retains the same intensity. In the IL $[C_4mpyr][Tf_2N]$, this stretching mode of the "free" anion appears at around 740 cm^{-1}.[44–59] As expected, upon coordination to a Lewis acid centre (here Mn^{2+}), the ν_s (S−N−S) frequency increases. The symmetric ν_s (S−O) stretching modes ($[C_2mim][Mn(Tf_2N)_3]$: ν_s (S−O) at 1145 cm^{-1}, $[C_3mim][Mn(Tf_2N)_3]$: ν_s (S−O) at 1139 cm^{-1}, $[C_4mim][Mn(Tf_2N)_3]$: ν_s (S−O) at 1143 cm^{-1}, and $[C_6mim][Mn(Tf_2N)_3]$: ν_s (S−O) at 1138 cm^{-1}; see Figure 2(e)) are also sensitive to

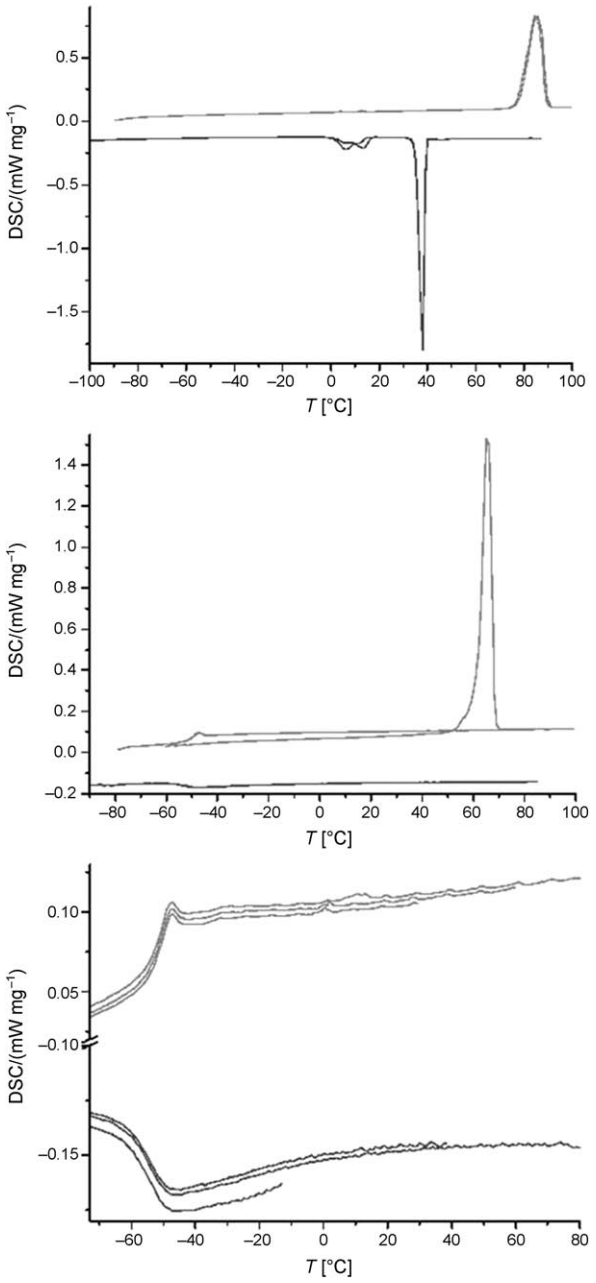

Figure 1. Representative thermograms of $[C_2mim]_2[MnCl_4]$ as a typical manganate(II) ionic liquid of class 1 (top), of $[C_4mim]_2[MnCl_4]$ as a typical manganate(II) ionic liquid of class 2 (middle), and of $[C_6mim]_2[MnCl_4]$ as a typical manganate(II) ionic liquid of class 3 (bottom). Heating cycle (upper curve); cooling cycle (lower curve), heating rate 5 K min^{-1}.

complexation to Lewis acid centres. Apparently, the S–O bond is weakened upon coordination of Tf_2N^- to Mn^{2+}. The S–O stretching modes appear in the same region as in homoleptic alkaline rare-earth Tf_2N compounds, but show no splitting, thus indicating only one coordination mode.[44] For comparison, Figure 2f shows the Raman spectra of HTf_2N and $Mn(Tf_2N)_2$. The symmetric stretching mode of the C–F bonds appears at the same wavenumber, supporting the view that this mode is not perturbed by the nature of the cation or its coordination mode. The ν_s (S–N–S) band deviates only slightly for the two components, whereas the ν_s (S–O) band of $Mn(Tf_2N)_2$ (1154 cm^{-1}) is shifted by about 18 cm^{-1} to lower wavelength compared to that of the free acid HTf_2N (ν_s (S–O) 1136 cm^{-1}) due to interactions of the oxygens of the SO_2 groups with the manganese Lewis acid centre.

Optical spectroscopy—general aspects: In the case of Mn^{2+}, its d^5 electronic configuration is its own hole equivalent. Thus, the Tanabe–Sugano[27,28] energy-level diagrams for both the tetrahedral and octahedral coordination modes are identical. To the first order approximation, the electronic states of Mn^{2+} are unperturbed by all nuclear motions that reduce symmetry. The upper ^4E, $^4A_1(G)$, and ^4E, $^4A_1(D)$ states and the $^6A_1$ state have the same slopes on the energy-level diagrams.[2] This accounts for the comparatively sharp lines observed for the $^6A_1 \rightarrow {}^4E$, $^4A_1(G)$ transition as well as the $^6A_1 \rightarrow {}^4A_1(D)$ transition in the absorption spectra.

Electric dipole transitions within high-spin (hs) centrosymmetric, octahedral Mn^{2+} complexes are both spin- and parity-forbidden, indicating a long lifetime of the excited electronic states. Non-centrosymmetric hs-Mn^{2+} compounds have Laporte-allowed d–d transitions, although these are still spin-forbidden. The emission decays of their excited states are generally lower by a factor of five compared to those of Mn^{2+} systems with an inversion centre.[29]

UV/Vis: The coordination environment of Mn^{2+} can be easily judged from the colour of the compound. Compounds with Mn^{2+} in a tetrahedral environment are usually yellow-greenish in colour, while those with octahedrally coordinated Mn^{2+} tend to be pale red or pink. Transitions observed in the range 300–800 nm can be assigned to the expected intraconfigurational transitions of the Mn^{2+} ion (Figure 3 and Supporting Information Figures 86–97).[4,62–75] For tetrahedrally coordinated Mn^{2+}, electronic transitions are Laporte-allowed and thus show higher absorbances than in the case of an octahedral environment (by a factor of 100). The UV/Vis spectra of the compounds investigated here proved to be in excellent agreement with those reported in the literature.[4,62–76] No significant impact of the counter cation on the colour of the compounds could be detected. Solid- and liquid-state absorption spectra of the Mn^{2+} ILs do not differ significantly. In agreement with a smaller ligand field splitting for the tetrahedral complex anions compared to the octahedral complex anions, electronic transitions of the MnX_4^{2-} compounds were found at longer wavelengths.

Typical UV/Vis spectra of representative tetrahedrally coordinated Mn^{2+} ILs are shown in Figure 3a and b. Two distinct groups of bands were observed in the UV/Vis region for all of the studied ILs. The first group of absorption bands may be attributed to transitions to D-term states with strong ligand field splitting, whereas the second group of bands originates from small ligand-field-split G-terms. In general, the bands of the G-terms appear with much lower intensities than those of the D-terms.

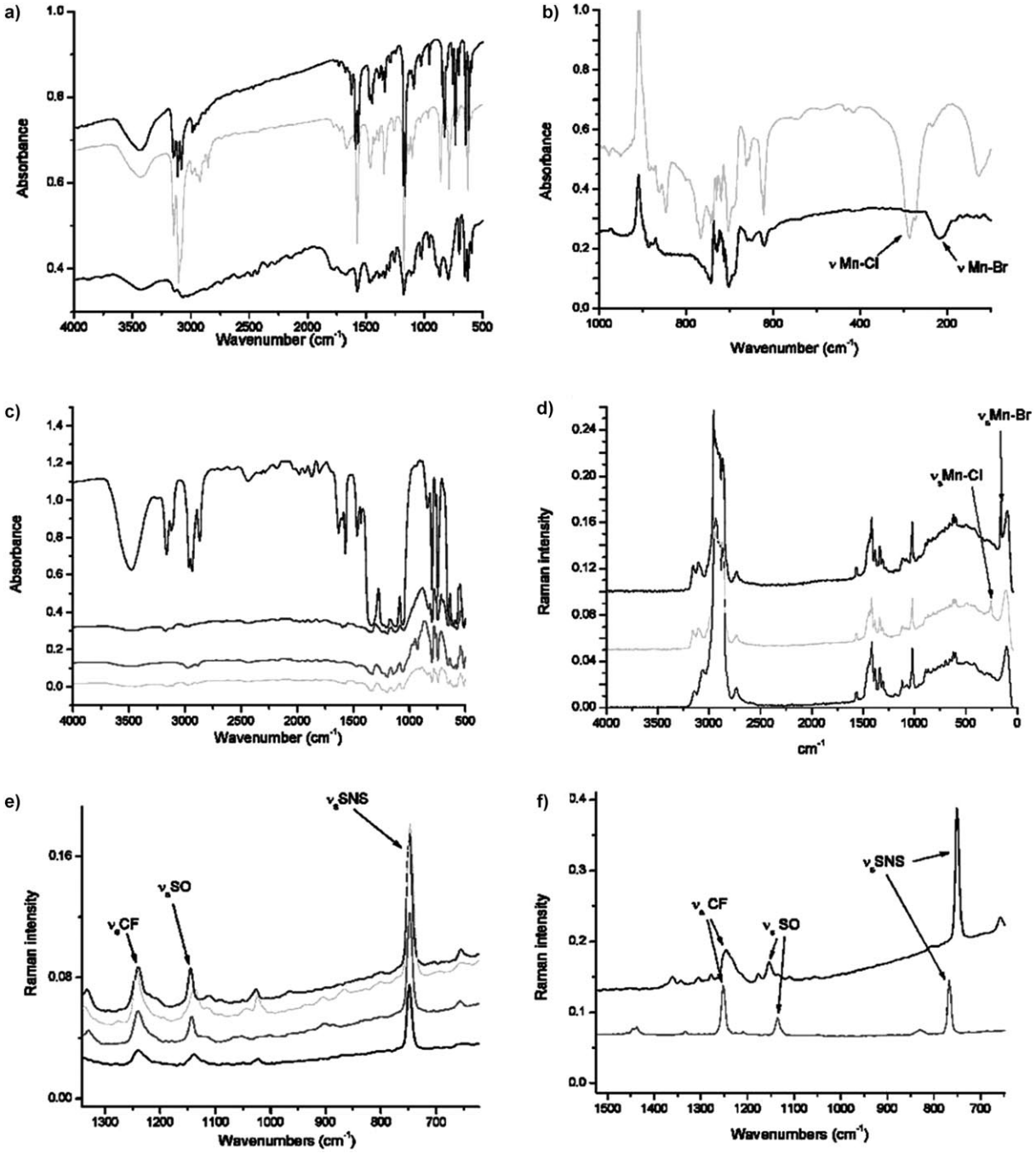

Figure 2. a) Mid-IR spectra of $[C_6mim]_2[MnBr_4]$ (top), $[C_2mim]_2[MnCl_4]$ (middle), and $[C_6mim]Br$ (bottom); b) far-IR spectra of $[C_6mim]_2[MnCl_4]$ (top) and $[C_6mim]_2[MnBr_4]$ (bottom); c) mid-IR spectra of $[C_2mim][Mn(Tf_2N)_3]$ (2nd from top), $[C_3mim][Mn(Tf_2N)_3]$ (bottom), $[C_4mim][Mn(Tf_2N)_3]$ (2nd from bottom), and $[C_6mim][Mn(Tf_2N)_3]$ (top); d) Raman spectra of $[C_6mim]_2[MnBr_4]$ (top), $[C_6mim]_2[MnCl_4]$ (middle), and $[C_6mim]Br$ (bottom); e) sections of the Raman spectra of $[C_2mim][Mn(Tf_2N)_3]$ (top), $[C_3mim][Mn(Tf_2N)_3]$ (2nd from top), $[C_4mim][Mn(Tf_2N)_3]$ (2nd from bottom), and $[C_6mim][Mn(Tf_2N)_3]$ (bottom); f) sections of the Raman spectra of $Mn(Tf_2N)_2$ (top) and HTf_2N (bottom).

For the tetrachloromanganates, the most intense band in the UV region corresponds to the $^6A_1 \rightarrow {}^4E(D)$ transition. Other bands are due to the very weak $^6A_1 \rightarrow {}^4T_2(D)$, the weak $^6A_1 \rightarrow {}^4A$, $^4E(G)$, and the intense $^6A_1 \rightarrow {}^4T_2(G)$ transitions. A broad feature at 470–475 nm is most likely an energy-transfer band, $^6A_1 \rightarrow {}^4T_1(G)$ (Table 2). In comparison with the tetrachloromanganates, for the tetrabromo analogues the $^6A_1 \rightarrow {}^4E(D)$ transition is generally of lower intensity than the $^6A_1 \rightarrow {}^4T_2(D)$ band and the absorption bands are blue-shifted by 2–6 nm. According to the Tanabe–Sugano diagram for d^5 ions, the $^6A_1 \rightarrow {}^4E(D)$ transition depends on the ligand field strength. Consequently, the electron-donor ability of the ligand can be estimated from the absorption maximum. As the absorption maxima of the tet-

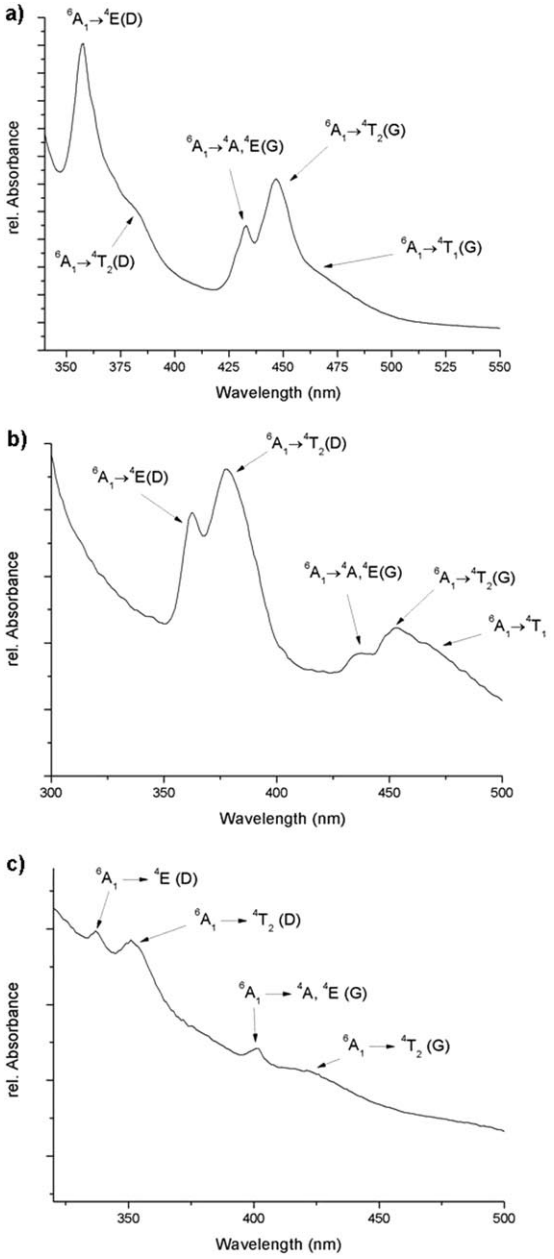

Figure 3. UV/Vis spectra of $[C_4mim]_2[MnCl_4]$ (a), $[C_4mim]_2[MnBr_4]$ (b), and $[C_3mim][Mn(Tf_2N)_3]$ (c).

rabromo compounds lie at lower wavelengths compared to those of the tetrachloromanganates, the tetrabromo compounds have a higher degree of covalency.

As the spectra of the solid ILs with complex Mn-Tf_2N cations showed a low signal-to-noise ratio, these ILs were diluted with the respective Mn-free IL for UV/Vis measurements (except in the case of the ethylimidazolium derivatives). Two discrete groups of bands were again observed (Figure 3c), one group consisting of two bands at 337 nm due to $^6A_1\rightarrow{}^4E(D)$ and at 351 nm due to $^6A_1\rightarrow{}^4T_2(D)$, and a second group at longer wavelengths with transitions at 401 nm due to $^6A_1\rightarrow{}^4A$, $^4E(G)$ and at 422 nm due to $^6A_1\rightarrow{}^4T_2(G)$ (Table 3). The observed electronic transitions are similar to those found for MnF_2,[77,78] in which Mn^{2+} is octahedrally coordinated by F.

Luminescence spectroscopy: Excitation and photoluminescence spectra were recorded at room temperature. The luminescence decay times were measured at room temperature and at the temperature of liquid nitrogen. For the C_3mim salts, the temperature dependence of the luminescence decay times was also investigated.

To record the excitation spectra, the emission intensity of the most intense transition was monitored while the excitation wavelength was continuously varied over the range 300 to 500 nm. In the excitation spectra (Figure 4, left, and the Supporting Information), the d-d transitions of the Mn^{2+} ion are clearly visible. These transitions can be assigned to the expected intraconfigurational transitions for a tetrahedrally (in the case of the halide compounds) or octahedrally (in the case of the Tf_2N compounds) coordinated Mn^{2+} ion.[77] The excitation spectra are in excellent agreement with the previously recorded UV/Vis spectra.

All emission spectra were recorded after direct excitation from the $^6A_1$ to the $^4E(D)$, $^4T_2(D)$ states of Mn^{2+}. These transitions are the most intense absorption bands in the UV region for each of the compounds. In the emission spectra, only one intraconfigurational transition can be observed between 400 and 700 nm (see the Supporting Information). In the case of tetrahedrally coordinated Mn^{2+}, the $^4T_1(G)\rightarrow{}^6A_1$ radiative transition is observed as a characteristic yellow-greenish emission at around 520 nm. For octahedrally coordinated Mn^{2+} compounds, the $^4T_1(G)\rightarrow{}^6A_1$ transition is observed with a reddish color at about 590 nm (see Table 4). All samples containing alkyl chains shorter than hexyl exhibit appreciably intense photoluminescence (see Figures 28–72 in the Supporting Information). Emission band half-widths of around 50 nm (200 cm^{-1}) were observed in all of the emission spectra. Appreciable shifts of the emission maxima depending on the counter cation were observed, especially for the chloro and bromo derivatives (see Table 4).

Table 2. Assigned transitions of the collected UV/Vis data of the tetrahalogenomanganate complexes. Wavelengths are in nm.

	$^6A_1\rightarrow{}^4E(D)$	$^6A_1\rightarrow{}^4T_2(D)$	$^6A_1\rightarrow{}^4A,\ {}^4E(G)$	$^6A_1\rightarrow{}^4T_2(G)$	$^6A_1\rightarrow{}^4T_1(G)$
$[C_2mim]_2[MnCl_4]$	357	381	433	446	472
$[C_3mim]_2[MnCl_4]$	358	381	433	447	470
$[C_4mim]_2[MnCl_4]$	358	383	433	447	470
$[C_6mim]_2[MnCl_4]$	358	381	433	446	472
$[C_2mim]_2[MnBr_4]$	362	380	435	453	470
$[C_3mim]_2[MnBr_4]$	362	379	435	452	471
$[C_4mim]_2[MnBr_4]$	362	377	436	453	470
$[C_6mim]_2[MnBr_4]$	363	380	436	454	472

Table 3. Assigned transitions of the collected UV/Vis data of the Tf_2N derivatives of the manganate complexes. Wavelengths are in nm.

	$^6A_{1g}\rightarrow{}^4E_g(D)$	$^6A_{1g}\rightarrow{}^4T_{2g}(D)$	$^6A_{1g}\rightarrow{}^4A_g$, $^4E_g(G)$	$^6A_{1g}\rightarrow{}^4T_{2g}(G)$
$[C_2mim][Mn(Tf_2N)_3]$	337	351	402	424
$[C_3mim][Mn(Tf_2N)_3]$	337	351	401	422
$[C_4mim][Mn(Tf_2N)_3]$	336	351	401	421
$[C_6mim][Mn(Tf_2N)_3]$	337	351	402	421

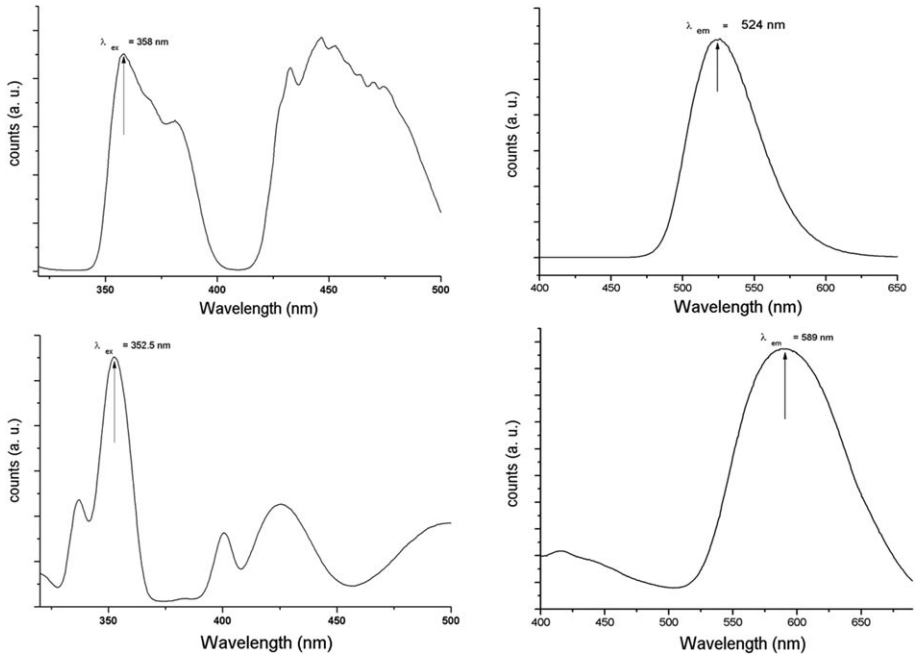

Figure 4. Excitation (left) and emission (right) spectra of $[C_2mim]_2[MnCl_4]$ (top) and $[C_2mim][Mn(Tf_2N)_3]$ (bottom).

Table 4. List of the observed emission maxima [nm] of the investigated manganese compounds at RT.

	Emission maximum [nm]		Emission maximum [nm]		Emission maximum [nm]
$[C_2mim]_2[MnCl_4]$	524	$[C_2mim]_2[MnBr_4]$	514	$[C_2mim][Mn(Tf_2N)_3]$	589
$[C_3mim]_2[MnCl_4]$	510	$[C_3mim]_2[MnBr_4]$	518	$[C_3mim][Mn(Tf_2N)_3]$	592
$[C_4mim]_2[MnCl_4]$	516	$[C_4mim]_2[MnBr_4]$	519	$[C_4mim][Mn(Tf_2N)_3]$	589
$[C_6mim]_2[MnCl_4]$	[a]	$[C_6mim]_2[MnBr_4]$	[a]	$[C_6mim][Mn(Tf_2N)_3]$	[a]

[a] Too weak to detect with the experimental set-up used.

Upon melting, all bands in the photoluminescence spectra shifted by about 10 nm (100–200 cm^{-1}) to lower wavelengths, indicating weaker intramolecular interactions.

The discrepancy between the Stokes shifts of the Mn^{II}-based halido derivatives and the NTf_2 derivatives stems from the symmetries and MO contributions of the respective ligands. The four halide ligands overlap more strongly with the manganese d-orbitals than the six weakly coordinating oxygens of the NTf_2 anions. Coordination of the latter is weaker due to symmetry aspects of the bond length and a lower overlapping contribution. The contrasting luminescences of the two series of ILs are illustrated in Figure 5.

Emission decay studies: The luminescence decay curves of the $^4T_1(G)\rightarrow{}^6A_1$ radiative transition were measured and a single exponential function could be fitted to the data, confirming that just one optical Mn^{2+} species was present. The experimental luminescence emission decays at room temperature and at −196 °C are compiled in Table 5. Upon melting or in the metastable liquid state at room temperature, no appreciable emission could be detected for the halogenido ILs due to vibrational quenching.[79]

The present tetrabromomanganates were found to exhibit emission decays of the excited Mn^{2+} states of about 0.4 ms at room temperature, which is in good agreement with literature values.[29] In contrast, the respective excited states of the tetrachloromanganate compounds persist for about 3 to 5 ms.[80–85] The higher degree of covalency in the complex bromides compared to the chlorides leads to a higher degree of vibronic coupling and hence to a reduction in the lifetime of the excited state. This assumption is supported by comparing the respective Mn–X modes in the vibrational spectra (see above).

To the best of our knowledge, the Tf_2N derivatives of the Mn ILs exhibit the longest reported phosphorescence decays of Mn^{2+}. These compounds have emission decays of about 30 ms (see Table 5). Generally, lifetimes of about 12–15 ms have been reported previously.[77] In these compounds in the crystalline solid state, the Mn^{2+} has octahedral site symmetry. The combined effect of the Laporte forbiddance and the spin-forbidden transitions leads to very long excited-state decay times of up to 25 ms at room temperature and 34 ms at 77 K for $[C_3mim][Mn(Tf_2N)_3]$. In the cases of the tetrachloro and tris[bis(trifluoromethanesulfonyl)amide]manganates, in which there is less covalent bonding between the metal and the ligand compared to the bromido compounds, the lifetimes are strongly temperature-dependent. Non-radiative deactivation processes are more likely to occur at higher temperatures. Consequently, the lifetimes of the ex-

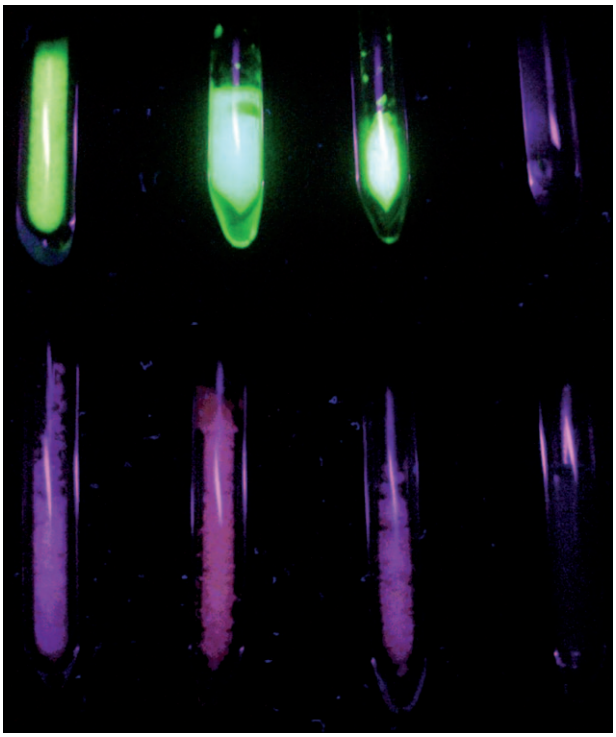

Figure 5. From left to right in the top row $[C_2mim]_2[MnCl_4]$, $[C_3mim]_2[MnCl_4]$, $[C_4mim]_2[MnCl_4]$, and $[C_6mim]_2[MnCl_4]$; in the bottom row $[C_2mim][Mn(Tf_2N)_3]$, $[C_3mim][Mn(Tf_2N)_3]$, $[C_4mim][Mn(Tf_2N)_3]$, and $[C_6mim][Mn(Tf_2N)_3]$ excited at room temperature with UV light (λ_{ex} = 366 nm).

Table 5. Emission decays of the Mn-based ILs at room temperature (RT) and at −196 °C (liquid nitrogen). Emission decay values are in ms.

	RT	−196 °C
$[C_2mim]_2[MnCl_4]$	1.5 (s)	3.4 (s)
$[C_3mim]_2[MnCl_4]$	4.6 (s)	5.5 (s)
$[C_4mim]_2[MnCl_4]$	3.9 (s)	4.2 (s)
$[C_6mim]_2[MnCl_4]$	(l)[a]	4.0 (s)
$[C_2mim]_2[MnBr_4]$	0.4 (s)	0.4 (s)
$[C_3mim]_2[MnBr_4]$	0.4 (s)	0.4 (s)
$[C_4mim]_2[MnBr_4]$	0.4 (s)	0.4 (s)
$[C_6mim]_2[MnBr_4]$	(l)[a]	0.4 (s)
$[C_2mim][Mn(Tf_2N)_3]$	22.8 (s)	29.7 (s)
$[C_3mim][Mn(Tf_2N)_3]$	24.8 (s)	33.9 (s)
$[C_4mim][Mn(Tf_2N)_3]$	18.8 (s)	32.4 (s)
$[C_6mim][Mn(Tf_2N)_3]$	(l)[a]	32.7 (s)
$Mn(Tf_2N)_2$	17.3 (s)	38.3 (s)

[a] Too weak/short-lived to detect with the experimental set-up used; s: solid; l: liquid.

cited states at 77 K are higher compared to those at 298 K. For the tetrabromomanganates, the lifetimes remain constant between 77 and 298 K. This observation is in agreement with studies on other tetrabromomanganates with organic counter cations.[86]

To study the temperature dependence of the lifetimes of the excited states in more detail for $[C_3mim]_2[MnCl_4]$, $[C_3mim]_2[MnBr_4]$, and $[C_3mim][Mn(Tf_2N)_3]$, the temperature dependences of the emission decays were determined

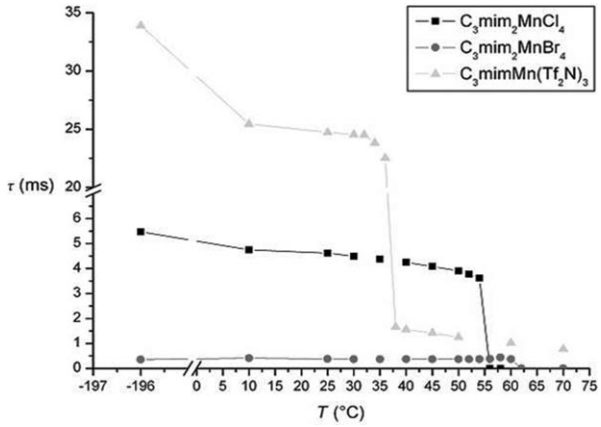

Figure 6. Temperature dependences of the emission decays of $[C_3mim]_2[MnCl_4]$, $[C_3mim]_2[MnBr_4]$, and $[C_3mim][Mn(Tf_2N)_3]$ upon melting.

in liquid nitrogen and in the temperature range from 10 °C to 70 °C in steps of 2–15 °C. Figure 6 shows the temperature dependences of the emission decays of the C_3mim compounds of Mn^{2+}.

Increasing temperature of the samples results in a decrease in the emission decay times of the excited $^4T_1(G)$ state due to thermal motion and vibration of the ions. Starting with the solid samples at 10 °C and increasing the temperature in steps of 2–15 °C, a sudden drop in the measured emission decay was seen at the melting point. In the case of the halogenido compounds, no luminescence could be detected, whereas for $[C_3mim][Mn(Tf_2N)_3]$ a weak reddish luminescence was observed. Deactivation through collisions resulting from thermal motion is attenuated by the Tf_2N anion, and this action is favoured by the octahedral site symmetry of Mn^{2+} in the Tf_2N complex.

Triboluminescence: Tetrahalogenomanganates are well-known emitters of tribo-induced radiation due to their piezoelectric properties, which can be excited through mechanical means when an applied electric field induces polarization of a suitable sample.[5,60,61] This results in a characteristic greenish emission when crystals of such Mn^{II} compounds are rubbed. Triboluminescence could be observed when crystals of the tetrahalogenido salts were rubbed with a glass rod. The light flashes emitted from the manganate complexes were greenish in colour and could be observed by the eye for only a fraction of a second.

Electroluminescence: When a high voltage was applied to solid samples of the Mn IL complexes, electroluminescence could be observed. As expected, the bromido and chlorido compounds showed a greenish luminescence, whereas the Tf_2N compounds emitted red light. No visible emission could be observed for any of the hexylimidazolium-containing samples.

Conclusions

We have reported the synthesis and optical properties of a series of imidazolium-based manganese(II)-containing ionic liquids. The imidazolium rings have been derivatized with *n*-alkyl chains from C_2 to C_6. All of these salts proved to be true ionic liquids, with melting points below 100 °C. Since all of these ILs are solid at room temperature, except for the hexyl derivatives, these compounds show luminescent properties in the visible region. However, the luminescence phenomena are completely quenched when the solid samples of the halogeno derivatives are melted because of thermal collision deactivation. In one case, we were able to observe luminescence phenomena in the liquid state.

The optical properties of the studied ILs were confirmed by comparison with literature values and were in excellent agreement with recent measurements. No significant perturbation of the optical properties of the luminescent manganese centre could be observed as a result of extending the alkyl chain at the imidazolium ring. When the local environment of the manganese centre is changed from tetrahedral to octahedral coordination site symmetry, the optical properties are strongly influenced. Tetrahedrally coordinated solid tetrabromo- and tetrachloromanganates exhibit intense greenish fluorescent and phosphorescent emissions, whilst solid Mn^{2+}-based ILs octahedrally coordinated by Tf_2N display weak reddish emissions. These emission phenomena could also be observed when solid samples were rubbed with a glass rod or excited by a high-voltage amplifier.

Depending on the local environment and the electron-donating abilities of the ligands, the emission decays of the excited states of Mn^{2+} vary from 0.4 ms up to more than 25 ms at room temperature. Low-temperature emission decay studies revealed that ligands with low donor abilities, such as the shielding Tf_2N, extend the emission decay of the excited Mn^{2+}-based IL, whereas the higher the electron donor ability the more abrupt the emission decay of the excited state will be. A phosphorescence emission decay of about 0.8 ms could even be observed in the case of molten $[C_3mim][Mn(Tf_2N)_3]$ at 70 °C. In the molten liquid state, $[C_3mim][Mn(Tf_2N)_3]$ shows very weak reddish light emission, proving that the Tf_2N anion is effective in shielding against thermal collision deactivation.

Acknowledgements

A.-V.M. thanks the Fonds der Chemischen Industrie for a Dozentenstipendium and the State of North-Rhine Westphalia and the Deutsche Forschungsgemeinschaft (SPP 1191) for generous financial support. The authors acknowledge Dr. Joanna Cybinska for re-measuring and confirming the photophysical properties. The authors wish to thank the reviewers for their valuable comments.

[1] H. W. Lawrence, *An Introduction to Luminescence of Solids*, Wiley, New York, **1950**.
[2] L. E. Orgel, *J. Chem. Phys.* **1955**, *23*, 1958.
[3] K. E. Lawson, *J. Chem. Phys.* **1967**, *47*, 3627.
[4] F. A. Cotton, D. M. L. Goodgame, M. Goodgame, *J. Am. Chem. Soc.* **1962**, *84*, 167.
[5] F. A. Cotton, *Inorg. Chem.* **2001**, *40*, 3576.
[6] K. Sato, M. Morita, S. Okamoto, S. Morita, T. Kambara, K. I. Gondaira, H. Takenoshita, *Prog. Cryst. Growth Charact.* **1984**, *10*, 311.
[7] G. O. Müller, *Phys. Status Solidi A* **1993**, *139*, 263.
[8] J. Benoit, *Phys. Status Solidi A* **1988**, *105*, 637.
[9] E. Chimczak, J. W. Allen, *J. Phys. D* **1985**, *18*, 951.
[10] M. F. Bulanyi, A. V. Kovalenko, B. A. Polezhaev, *Inorg. Mater.* **2002**, *36*, 222.
[11] N. T. Gurin, O. Y. Sabitov, *Tech. Phys.* **2006**, *51*, 1012.
[12] B. Mallick, Diploma Thesis, University of Cologne (Cologne), **2007**.
[13] S. Hayashi, H. Hamaguchi, *Chem. Lett.* **2004**, *33*, 1590.
[14] Y. Yoshida, A. Otsuka, G. Saito, S. Natsume, E. Nishibori, M. Takata, M. Sakata, T. Yoko, *Bull. Chem. Soc. Jpn.* **2005**, *78*, 1921.
[15] Y. Yoshida, G. Saito, *J. Mater. Chem.* **2006**, *16*, 1254.
[16] C. Zhong, T. Sasaki, A. J. Kobayashi, E. Fujiwara, A. Kobayashi, Y. Iwasawa, *Bull. Chem. Soc. Jpn.* **2007**, *80*, 2365.
[17] R. Del Sesto, P. Williams, *Chem. Commun.* **2008**, 447.
[18] N. Sabbatini, M. Guardigli, J.-M. Lehn, *Coord. Chem. Rev.* **1993**, *123*, 201.
[19] P. Wasserscheid, T. Welton, *Ionic Liquids in Synthesis, Vol. 1*, Wiley-VCH, Weinheim, **2002**.
[20] K. Seddon, M. Earle, WO2006043110 (A1), United Kingdom, **2006**.
[21] A. Babai, A.-V. Mudring, *Chem. Mater.* **2005**, *17*, 6230.
[22] S. Tang, A. Babai, A.-V. Mudring, *Angew. Chem.* **2008**, *120*, 7743; *Angew. Chem. Int. Ed.* **2008**, *47*, 7631.
[23] B. Mallick, B. Balke, C. Felser, A.-V. Mudring, *Angew. Chem.* **2008**, *120*, 7747; *Angew. Chem. Int. Ed.* **2008**, *47*, 7635.
[24] A. Babai, S. Arenz, R. Giernoth, K. Driesen, P. Nockemann, A.-V. Mudring, *J. Alloys Compd.* **2005**, *386–406*, 204.
[25] S. Arenz, A. Babai, K. Binnemans, K. Driesen, R. Giernoth, A.-V. Mudring, *Chem. Phys. Lett.* **2005**, *402*, 75.
[26] G. H. Dieke, *Spectra and Energy Levels of Rare Earth Ions in Crystals*, Interscience Publishers, New York, **1968**.
[27] Y. Tanabe, S. Sugano, *J. Phys. Soc. Jpn.* **1954**, *9*, 766.
[28] Y. Tanabe, S. Sugano, *J. Phys. Soc. Jpn.* **1954**, *9*, 753.
[29] K. Vögtle, Ph.D. Thesis, University of Karlsruhe (Karlsruhe), **1982**.
[30] C. P. Fredlake, J. M. Crosthwaite, J. F. Brennecke, *J. Chem. Eng. Data* **2004**, *49*, 954.
[31] M. J. Gall, M. J. Ware, *Spectrochim. Acta* **1970**, *26A*, 287.
[32] H. D. Lutz, H. J. Schneider, *Z. Anorg. Allg. Chem.* **1991**, 592.
[33] F. Guillaume, A. J. Dianoux, *J. Chem. Phys.* **1990**, *92–93*, 3438.
[34] R. Callaghan, O. Siiman, *Inorg. Chem.* **1981**, *20*, 1723.
[35] Y. Jeon, D. Kim, *J. Phys. Chem. B* **2008**, *112*, 4735.
[36] Y. Jeon, D. Kim, *J. Chem. Phys.* **2008**, *128-129*, 928.
[37] P. W. W. Hunter, G. A. Webb, *J. Inorg. Nucl. Chem.* **1972**, *34*, 1511.
[38] A. Lucken, H. Bill, *J. Phys. Condens. Matter* **1991**, *3*, 5085.
[39] H. G. M. Edwards, L. A. Woodward, *Chem. Commun.* **1968**, 541.
[40] J. S. Avery, D. M. L. Goodgame, *Spectrochim. Acta* **1967**, *24A*, 1721.
[41] K. Wussow, H. D. Lütz, *J. Solid State Chem.* **1989**, *78*, 117.
[42] A. R. Parent, M. M. Trulli, *Inorg. Chim. Acta* **2007**, *360*, 1943.
[43] J. Weidlein, U. Müller, K. Dehnicke, *Schwingungsfrequenzen II, Vol. 1*, Thieme, Stuttgart, **1986**.
[44] A. Babai, A.-V. Mudring, *Inorg. Chem.* **2006**, *45*, 3249.
[45] M. Castriota, T. Caruso, *J. Phys. Chem. A* **2005**, *109*, 92.
[46] I. Rey, L. Servant, *Electrochim. Acta* **1998**, *43*, 1505.
[47] K. Fujii, S. Ishiguro, *J. Phys. Chem. B* **2007**, *111*, 12829.
[48] S. Riviera-Rubero, S. Baldelli, *J. Chem. Phys.* **2006**, *124-125*, 4756.
[49] L. J. Hardwick, P. Novak, *J. Raman Spectrosc.* **2007**, *38*, 110.
[50] J. C. Lassègues, P. Johansson, *J. Raman Spectrosc.* **2007**, *38*, 551.
[51] A. Bakker, K. Hermansson, *Polymer* **1995**, *36*, 4371.
[52] K. Iwata, H. Hamaguchi, *Acc. Chem. Res.* **2007**, *40*, 1174.
[53] P. A. Madden, F. Hutchinson, *J. Chem. Phys.* **2003**, *118–119*, 6609.
[54] R. Ozawa, H. Hamaguchi, *Chem. Lett.* **2003**, *32*, 948.
[55] S. A. Katsyuba, A. Vidiis, *Helv. Chim. Acta* **2004**, *87*, 2556.
[56] R. W. Berg, J. M. Thompson, *J. Chem. Phys.* **2005**, *122–123*, 19018.
[57] H.-C. Chang, S. H. Liu, *J. Chem. Phys.* **2007**, *126–127*, 9201.
[58] A. Blaschette, H. Bürger, *Z. Anorg. Allg. Chem.* **1970**, *378*, 104.

[59] E. R. Talaty, W. R. Carper, *J. Chem. Phys.* **2004**, *120-121*, 13177.
[60] P. A. Thiessen, K. Meyer, *Naturwissenschaften* **1970**, *57*, 423.
[61] G. E. Hardy, J. I. Zink, *Inorg. Chem.* **1976**, *15*, 3061.
[62] N. Islam, *Appl. Spectrosc.* **1975**, *29*, 266.
[63] M. T. Vala, S. L. Holt, *Mol. Phys.* **1972**, *23*, 217.
[64] A. J. MacFarlane, R. J. P. Williams, *J. Chem. Soc. A* **1969**, 1519.
[65] J. J. Foster, N. S. Gill, *J. Chem. Soc. A* **1968**, 2625.
[66] C. Furlani, A. Furlani, *J. Inorg. Nucl. Chem.* **1961**, *19*, 51.
[67] S. J. Chan, H. Lütje, *J. Chem. Phys.* **1967**, *47*, 2121.
[68] A. Mehra, P. Venkateswarlu, *J. Chem. Phys.* **1966**, *45*, 3381.
[69] S. Buffagni, T. M. Dunn, *Nature* **1960**, *188*, 937.
[70] R. Lissilour, M. A. Makhyoun, *J. Chim. Phys.* **1981**, *78*, 335.
[71] D. Oelkrug, A. Wölpl, *Ber. Bunsen-Ges.* **1972**, *76*, 680.
[72] R. Parrot, K. Nikolic, *J. Lumin.* **1979**, *18*, 154.
[73] W. D. Perry, L. M. Vallerino, *Inorg. Chim. Acta* **1973**, *7*, 175.
[74] R. Pappalardo, *J. Chem. Phys.* **1959**, *31*, 1050.
[75] C. Naud, R. Parrot, *Phys. Rev. B* **1979**, *20*, 3333.
[76] V. Gutmann, K. Fenkart, *Monatsh. Chem.* **1966**, *45*, 286.
[77] G. Blasse, C. Grabmaier, *Luminescent Materials*, Springer, Berlin, **1994**.
[78] P. Manning, *Can. Mineral.* **1969**, *9*, 237.
[79] L. Burlamacchi, E. Tiezzi, *J. Phys. Chem.* **1970**, *74*, 3980.
[80] M. D. C. M. d. Lucas, M. Lorenzo, *Ferroelectrics* **1990**, *109*, 21.
[81] N. Presser, B. R. Sundheim, *Chem. Phys.* **1978**, *31*, 281.
[82] B. R. Sundheim, B. Howard, *J. Chem. Phys.* **1972**, *57*, 4492.
[83] B. R. Sundheim, J. L. Painter, *J. Coord. Chem.* **1984**, *13*, 185.
[84] K. Nikolic, F. Lignou, *J. Lumin.* **1973**, *8*, 137.
[85] M. Whrigton, D. Ginley, *Chem. Phys.* **1974**, *4*, 295.
[86] N. Presser, M. Ratner, B. R. Sundheim, *Chem. Phys. Lett.* **1977**, *45*, 572.

Received: December 17, 2008
Revised: October 21, 2009
Published online: February 4, 2010

